



HAL
open science

Fine Control of the Metal Environment within Dysprosium-Based Mononuclear Single-Molecule Magnets

D. Guettas, V. Montigaud, G.F. Garcia, P. Larini, O. Cador, Boris Le
Guennic, G. Pilet

► **To cite this version:**

D. Guettas, V. Montigaud, G.F. Garcia, P. Larini, O. Cador, et al.. Fine Control of the Metal Environment within Dysprosium-Based Mononuclear Single-Molecule Magnets. *European Journal of Inorganic Chemistry*, 2018, 2018 (3), pp.333-339. 10.1002/ejic.201701106 . hal-01713495

HAL Id: hal-01713495

<https://univ-rennes.hal.science/hal-01713495v1>

Submitted on 15 Apr 2021

HAL is a multi-disciplinary open access archive for the deposit and dissemination of scientific research documents, whether they are published or not. The documents may come from teaching and research institutions in France or abroad, or from public or private research centers.

L'archive ouverte pluridisciplinaire **HAL**, est destinée au dépôt et à la diffusion de documents scientifiques de niveau recherche, publiés ou non, émanant des établissements d'enseignement et de recherche français ou étrangers, des laboratoires publics ou privés.

Fine control of metal environment within dysprosium-based mononuclear Single-Molecule Magnets

Djamila Guettas,^[a] Vincent Montigaud,^[b] Guglielmo Fernandez Garcia,^[b,c] Paolo Larini,^[d] Olivier Cador,^[b] Boris Le Guennic^[b] and Guillaume Pilet^{*[a]}

Molecular Magnetism - The Attractive Legacy of Olivier Kahn

Abstract: A new family of three Dy(III) mononuclear complexes and one Dy(III) chain system based on the same ligand (1,3-di(pyridin-4-yl)propane-1,3-dione) has been isolated as single-crystals. By varying the synthesis conditions, it has been possible to finely control the number of ligands coordinated to the central lanthanide atom (from 1 to 3) and then the total charge of the complex unit (from +2 to neutral) as well as the local geometry around the Dy(III) ion (from D_{4d} to D_{2d}). The magnetic properties of the four complexes have been studied and rationalized by *ab initio* calculations in order to illustrate the correlation between the metal ion environment, due to the number of coordinated ligands, and their SMM behaviours.

Introduction

Since three decades that Single-Molecule Magnets (SMMs) have been discovered,^[1] many ways to synthesize them have been explored and hundreds of SMMs have been published.^[2] The use of lanthanide ions represents an efficient strategy due to their significant magnetic anisotropy arising from the large unquenched orbital angular momentum. It generates an intense field of research especially in the field of mononuclear SMMs (known also as Single-Ion Magnets (SIMs)).^[3] The slow relaxation of the magnetization in this special class of molecules arises from a single metal centre. In such complexes, despite the limited total number of unpaired electrons, the intrinsic magnetic anisotropy can be significant leading to

mononuclear complexes with remarkably high energy barriers.^[4] In the latter, reversal of the magnetic moment is achieved either by thermal activation and/or Quantum Tunnelling of the Magnetization (QTM). Furthermore, it has been shown that the relaxing rates are extremely sensitive to tiny distortions of the coordination geometry in 4f-systems.^[5] Therefore, the design of novel structures is needed to enlarge the available database and thus to improve our knowledge on the structure-property relationship of lanthanide-containing mononuclear SMMs.

In this line, a successful modulation of SMMs properties has been performed recently by varying the auxiliary ligands in β -diketone-based Dy(III) complexes.^[6] This study highlights the meticulous choice of the ancillary ligand as a promising new path toward the design of new complexes exhibiting higher SMM characteristics. Moreover, theoretical studies performed on these complexes have shown that mixing charged ligands and neutral ligands with Dy(III) adopting heteroleptic coordination mode may be a key to improve the magnetic behavior.^[7]

Based on this previous work that brings elements for the understanding of structure-property relationship, we have been interested in the study of a new series of β -diketone-based Dy(III) complexes with distinct metal ion coordination environment by varying the number of β -diketone ligands around the metal centre. Indeed, four original complexes, three mononuclear ones and one 1D polymer system, have been isolated by controlling the synthesis conditions (temperature, time, pressure ...) but using the same ligand. This leads to a finely controlled number of coordinated ligands around the Dy(III) centre which has an influence on the metal geometry environment. Their synthesis, crystal structures, magnetic properties supported by *ab initio* calculations are discussed in this article.

Results and Discussion

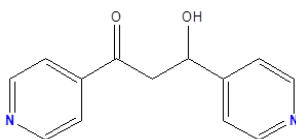
Syntheses. All the complexes were synthesized from the Dy(III) chloride hexahydrate salt using methanol as solvent. The ligand used (Scheme 1) is 1,3-di(pyridin-4-yl)propane-1,3-dione (HL_{NN}).^[8] This organic molecule is composed of a β -diketone fragment functionalized by two pyridine groups with nitrogen atoms in *para* position. Yellow crystals containing the complexes are obtained by slow evaporation of the solvent from the reaction mixture.

[a] D. Guettas, G. Pilet
Université de Lyon, Laboratoire des Multimatériaux et Interfaces (LMI), UMR 5615 CNRS-Université Claude Bernard Lyon 1
Bâtiment Chevreul, avenue du 11 novembre 1918, 69622
Villeurbanne cedex, France
guillaume.pilet@univ-lyon1.fr

[b] V. Montigaud, G. Fernandez Garcia, O. Cador, B. Le Guennic
Institut des Sciences Chimiques de Rennes, UMR 6226 CNRS-
Université de Rennes 1
263 avenue du Général Leclerc, 35042 Rennes cedex, France

[c] G. Fernandez Garcia
Dipartimento di Chimica, Università di Firenze, Via della Lastruccia
3 Polo Scientifico, 50019 Sesto fiorentino, Italy

[d] Paolo Larini
Université Lyon 1, CNRS, INSA, CPE, UMR 5246, ICBMS, ITEM, M,
43 Bd du 11 novembre 1918, F-69622 Villeurbanne, France



Scheme 1. HLNN ligand.

A series of mononuclear complexes was formed mainly by variation of temperature, pressure and reaction time during the different syntheses. Indeed, the four complexes were synthesized from the reaction mixtures containing identical proportions of reagents. In order to form the complex **3**, three equivalents of triethylamine are added, with stirring, to a mixture composed of one equivalent of the metal salt and two equivalents of the ligand in methanol. In the above proportions, refluxing the mixture during 48h allows to form complex **2**. By maintaining the same stoichiometry, complex **4**, a 1D molecular system, is synthesized under solvothermal conditions (70°C for 12h). Finally, in the above proportions, leaving the solution with stirring for 6h, a mixture of complexes **3** and **1** is obtained. On the other hand, when the quantity of the reactants is stoichiometric, with the same stirring time (6h), complex **1** is isolated as pure sample.

Crystal structure Analysis. Data collection details and refinement results are summarized in Supplementary Information (Table SI.1). Details on bond lengths, bond angles and distances within the structures can be found in Tables SI.2, SI.3, SI.4 and SI.5 for complexes **1**, **2**, **3** and **4**, respectively.

[Dy(L_{NN})(H₂O)₆]Cl₂·2H₂O (1**).** The complex **1** crystallizes in the centrosymmetrical monoclinic I2/a space group. The mononuclear entity [Dy(L_{NN})(H₂O)₆]²⁺ is a dication where the Dy(III) central ion is coordinated to one deprotonated L_{NN}⁻ ligand and six water molecules (Figure 1a). The charge balance is ensured by two chlorine counter-anions statistically distributed on three independent crystallographic positions. Two non-coordinated water molecules co-crystallize within the unit-cell and are statistically distributed on four crystallographic positions. With this configuration, the Dy(III) ion is located in a {O₈} environment with a distorted D_{4d} geometry (square anti-prism, Table SI.6).^[9] The Dy-O(L_{NN}) bond lengths (average of 2.288 Å) are shorter than the Dy-O(H₂O) ones (average of 2.385 Å). Due to π-π interactions between aromatic rings of ligands belonging to two neighbouring cationic units, pseudo-chains of complexes are formed along the [101] direction with complexes organized in a head-to-tail configuration (Figure SI.5). Within these pseudo-chains, the shortest Dy···Dy distance is 6.7 Å. The structural cohesion between the pseudo-chains is ensured by hydrogen bonds between coordinated and non-coordinated water molecules, between coordinated water molecules and chlorine anions and between nitrogen atoms from L_{NN}⁻ ligands and non-coordinated water molecules. Surprisingly, the shortest Dy···Dy distance between chains (6.9 Å) is only slightly longer than those within the chains.

[Dy(L_{NN})₂(MeOH)₂(H₂O)₆]Cl (2**).** The complex **2** crystallizes in the tetragonal P42/n space group. The refined structure reveals the presence in the unit-cell of one cationic entity,

[Dy(L_{NN})₂(MeOH)₂(H₂O)₂]⁺, composed by one Dy(III) ion coordinated to two deprotonated L_{NN}⁻ ligands, two methanol molecules and two water molecules (Figure 1b). The charge balance is ensured by the presence of one chlorine atom per cationic entity. Due to the coordination mode, the lanthanide centre is located in a {O₈} environment exhibiting a distorted D_{2d} local geometry (triangular dodecahedron, Table SI.6).^[9] Dy-O(L_{NN}) (2.340 Å, slightly longer than those observed in complex **1**) and Dy-O(H₂O) (2.376 Å) bond lengths are comparable within this structure. Finally, the Dy-O(MeOH) (2.424 Å) are the longest Dy-O bond lengths in this {DyO₈} environment. The molecular packing of each mononuclear complex leads to cavities running along the [001] direction (Figure SI.6) and exhibiting a diameter of 8 Å where Cl⁻ anions are inserted. The structural cohesion to form these cavities is built from plans of complexes with π-π interactions between aromatic rings of L_{NN}⁻ ligands belonging to two neighbouring cationic complexes. Within these plans, the shortest Dy···Dy distance is 11.0 Å. These cationic plans stack perfectly one above the other, linked together by hydrogen bonds involving coordinated water molecules and chlorine anions. The distance between two consecutive plans is 7.7 Å.

[Dy(L_{NN})₃(MeOH)₂] (3**).** The complex **3** crystallizes in the monoclinic P2₁/n space group. This is a neutral mononuclear complex composed by one Dy(III) cation coordinated to three deprotonated L_{NN}⁻ ligands and two methanol molecules (Figure 1c). The metal centre is then located in a {O₈} environment with a slightly distorted D_{4d} local geometry (square anti-prism, Table SI.6).^[9] Dy-O(L_{NN}) bond lengths within **3** (average of 2.381 Å) are comparable to those encountered for complex **2** but longer than those observed for complex **1**. Dy-O(MeOH) bond lengths in **3** are identical (+0.025 Å) to those in **2**. Complexes are organized as plans perpendicularly to the [100] direction in which the structural cohesion is ensured by π-π interactions between aromatic rings of L_{NN}⁻ ligands belonging to two neighbouring complexes (Figure SI.7). The shortest Dy···Dy distance between two complexes within this plan is 7.8 Å. These plans stack perfectly one above the other along the [010] direction with π-π interactions ensuring the global structural cohesion. The shortest Dy···Dy distance between two consecutive plans is 11.0 Å.

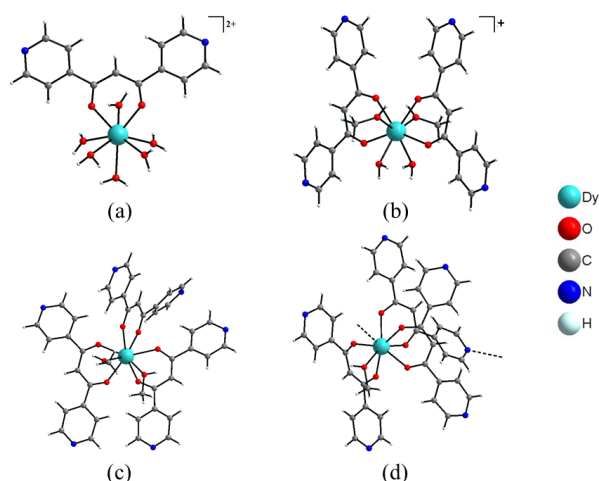


Figure 1. Representation of the molecular structure of complexes **1** (a), **2** (b) **3** (c) and **4** (d). Hydrogen atoms are omitted for clarity. In case of **4**, black dashed lines represent bridges between mononuclear units composing the 1D polymer.

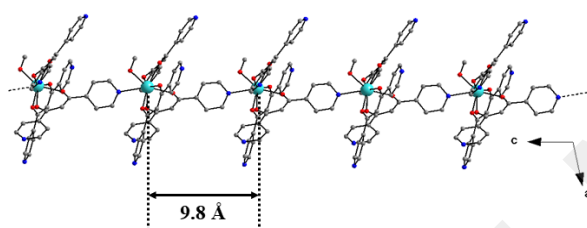


Figure 2. Chain of **4** running along the [001] direction of the unit-cell. For clarity, hydrogen atoms have been omitted. The distance between two dysprosium atoms belonging to two neighbouring units is highlighted.

{Dy(L_{NN})₃(MeOH)}_n·nH₂O (4**).** This complex crystallizes in the monoclinic system and its structure has been refined using the C2/c space group. The complex, exhibiting the following refined formula {Dy(L_{NN})₃(MeOH)}_n·nH₂O, is a 1D polymer running along the [001] direction (Figure 2). The asymmetric unit (Figure 1d) is composed by one Dy(III) cation coordinated to three deprotonated L_{NN}⁻ ligands and one coordinated methanol molecule. The lanthanide ion is then surrounded by seven

oxygen atoms and one nitrogen atom belonging to a L_{NN}⁻ ligand of a neighbouring complex unit. These Dy-N bonds between two consecutive sub-units form chains. Dy-O(L_{NN}) (average of 2.341 Å) are comparable to those observed for the complexes described above while the Dy-O(MeOH) bond length is longer (2.446 Å). As expected, the Dy-N(L_{NN}) bond length is also longer (2.602 Å) compared to the Dy-O ones. The Dy(III) ion is thus located in a {O₇N} coordination sphere adopting a D_{2d} distorted local geometry (triangular dodecahedron, Table SI.6).^[9] Within the chain, the shortest Dy···Dy distance is 9.8 Å. These chains stack perfectly one above the others perpendicularly to the [001] direction (Figure SI.8). The shortest Dy···Dy distance between two chains is 8.9 Å. The structural cohesion within plans is ensured by π - π interactions between aromatic ligands of two neighbouring chains. The shortest Dy···Dy distance between two consecutive plans is longer than those detailed above and equal to 10.0 Å.

Magnetic properties

Direct current (dc) magnetic susceptibility studies of **1-4** were carried out with an applied magnetic field of 1000 Oe over the temperature range 300-2 K. The plot of χT vs T, with χ the molar magnetic susceptibility and T the temperature in Kelvin, is shown in Figure 3. At room temperature the χT values (14.07, 13.95, 14.03 and 13.87 cm³ K mol⁻¹ for complexes **1** to **4**, respectively) are close to what is expected for the ⁶H_{15/2} multiplet ground state (14.17 cm³ K mol⁻¹) of Dy(III). χT 's decrease on cooling to reach 11.77, 10.92, 10.91 and 12.03 cm³ K mol⁻¹ at 2 K for **1** to **4**, respectively. The decrease of χT values can be ascribed to thermal depopulation of the Stark levels of the Dy(III) ions and/or to antiferromagnetic interactions between the spin carriers, as observed in other dysprosium complexes.^[10] Magnetization plots (M vs H) for **1-4** was measured at 2 K (Figure SI.9). The curves show a very similar behavior for all complexes: increase of the M values with the field H to reach saturation in the vicinity of 2 T. The corresponding values are 5.28 μ B, 5.08 μ B, 5.08 μ B and 5.09 μ B for **1-4**, respectively. These values appear to be very low compared to those expected in the free ion model (saturation at 10 μ B).^[11] Such low saturation values are often the sign of the presence of a large anisotropy within the complex with the stabilization of the Ising components $M_J = \pm 15/2$.^[12] This suggests, therefore, that complexes **1-4** could behave as mononuclear SMMs.

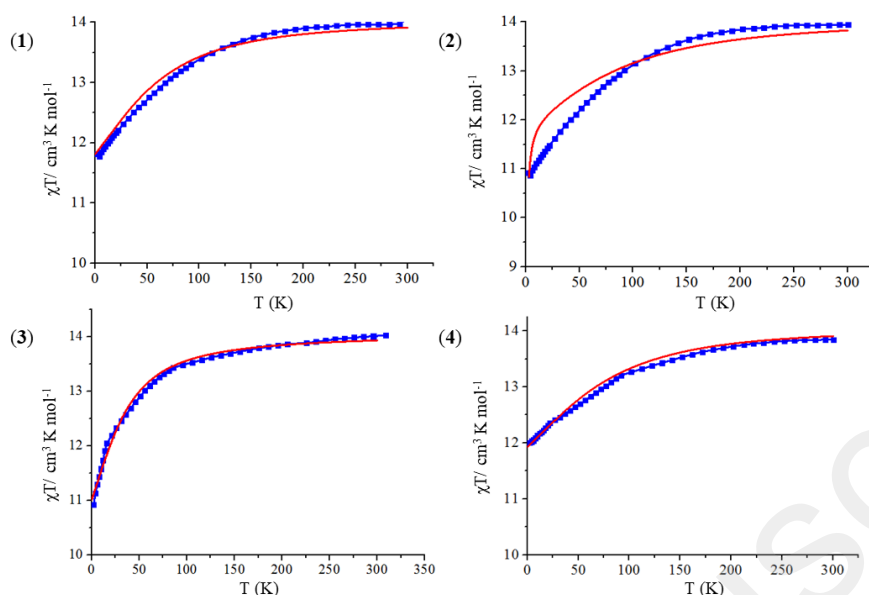


Figure 3. Plots of χT vs T values for complexes **1**, **2**, **3** and **4**. In insert are given the corresponding magnetization curves at 2 K. The calculated curves are represented in full red line.

In order to explore potential mononuclear SMM behaviour, alternating current (ac) magnetic susceptibility studies were carried out for complexes **1-4**. The in-phase (χ') and out-of-phase (χ'') susceptibilities were measured as a function of temperature at different frequencies in zero external dc field. χ'' plots show a frequency dependent signal for all complexes below 10 K (Figures Si.10 and Si.11). The low χ'' values for **2** and **3** with respect to **1** and **4** suggest that these two complexes relax faster than **1** and **4**. In all cases, the relaxation is fast and therefore the relaxation time, τ , of the systems cannot be monitored. This behaviour is generally induced by QTM which can be, at least partially, suppressed by an external dc field. Therefore, ac susceptibility measurements were performed at the optimum field, 1 kOe (Figure 4 and Figure Si.12).

By fitting the data with an Arrhenius law ($\tau = \tau_0 \exp(\Delta/kT)$) where τ_0 is the characteristic relaxation time and Δ is the activation energy for spin reversal, Figure Si.13), the effective barrier was evaluated at 76.5 K and the pre-exponential factor (τ_0) at 1.1×10^{-7} s for **1**; 55.0 K and 8.3×10^{-7} s for **2**; 44.8 K and 7.0×10^{-7} s for **3**; 40.8 K and 7.0×10^{-7} s for **4**. Normalized Cole-Cole and extended Debye analyses (Figure Si.14) give rise to different types of semi-circles (more or less distorted) leading to large values of the α parameter at high temperatures (0.91 for **1**, 0.86 for **2**, 0.82 for **3** and **4**).^[13] These large values and the asymmetry of the Cole-Cole curves might suggest the overlap of multiple relaxation processes.^[14] At lower temperature (3 K), α values strongly decrease to reach values of 0.12 for **1**, 0.14 for **2**, 0.23 for **3** and 0.13 for **4** indicating a moderate distribution of the relaxation time.

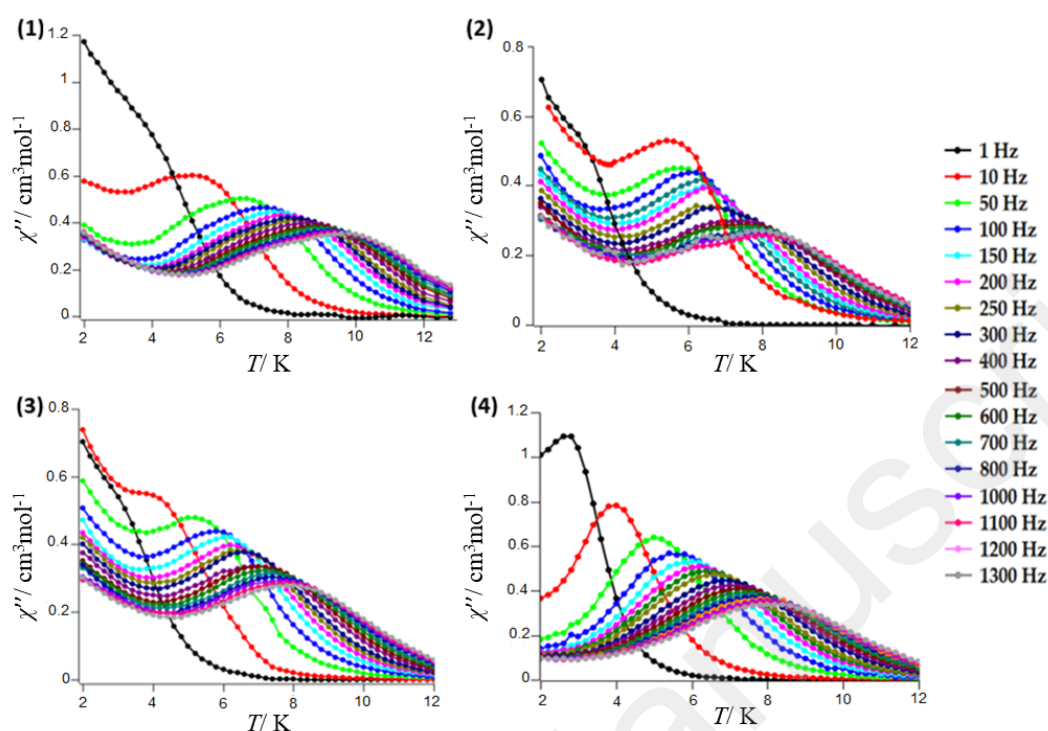


Figure 4. Plots of χ'' vs T values depending on frequencies at 1 kOe for complexes **1**, **2**, **3** and **4**.

Ab initio calculations

SA-CASSCF/SI-SO calculations were carried out on complexes **1-4** to give insights into the experimental magnetic behaviour (see computational details in the Experimental Section). In the case of complex **4**, the 1D arrangement was mimicked using LoProp charges calculated on the molecular fragment. Computed energies, g-tensor and wavefunction composition of the ground multiplet in the effective spin $\frac{1}{2}$ model are given in Tables SI.7-SI.10 for complexes **1-4**, respectively. Calculated magnetic axes are shown in Figure SI.15 whereas Figures SI.16-SI.19 give elements to magnetic relaxation, without taking into account phonons-driven mechanisms.^[15] All complexes are characterized by large $m_J = |\pm 15/2\rangle$ ground state with the first Kramers doublet lying 125, 192, 76 and 201 cm^{-1} higher in energy for complexes **1-4**, respectively. Ground state magnetic easy axes are as expected for Dy(III) ions along the most negatively charged directions. Experimentally, **2** and **3** relax faster (at zero dc field) than **1** and **4**. This is clearly supported by the calculations since i) the wavefunction of the ground KD of **3** has non-negligible $m_J = |\pm 11/2\rangle$ component inducing a least Ising magnetic anisotropy (Table SI.9) and ii) **2** and **3** show larger matrix elements connecting the $m_J = |\pm 15/2\rangle$ states than **1** and **4**. One should notice that there is no obvious correlation between the calculated energy difference between the ground

and first excited state and the evaluated experimental energy barrier.

Conclusions

In conclusions, four new Dy(III)-based complexes, three mononuclear ones and one chain system, have been synthesized using the same ligand. Depending on the synthesis conditions, it has been possible to finely control the number of coordinated ligands around the lanthanide ion and thus the local geometry around the metal cation. Magnetic measurements as well as *ab initio* calculations highlight the influence of this *4f* environment on the SMM behaviour for these four complexes. Overall, complex **1** (only one coordinated ligand, D_{4d} local geometry around the Dy(III) centre) is the best mononuclear SMM system ($\Delta = 76.5$ K) of the four complexes presented in this article.

Experimental Section

Syntheses. All reagents were purchased from Aldrich and used without further purification.

Synthesis of 1,3-di (pyridin-4-yl) propane-1,3-dione (HL_{NN}). To a suspension of 0.35 g of NaH (15 mmol, 3 equivalents) in 50 mL of

anhydrous tetrahydrofuran was added a solution of 0.72 g of 4-acetylpyridine (6 mmol, 1.2 equivalents). The mixture was kept under stirring and inert atmosphere at room temperature for 1h. Then 0.75 g (5 mmol, 1 equivalent) of methyl isonicotinate was added and the reaction mixture was left under stirring for 28h at 70°C. Water was finally added to the solution. After neutralization of the mixture with glacial acetic acid, 0.62 g of a yellowish solid is collected (yield = 86%) NMR ¹H (CDCl₃, 300 MHz) δ (ppm): 15.43 (s, 1H); 8.84 (dd, J = 8.65 Hz, 4H); 8.03 (dd, J = 8.62 Hz, 4H); 7.46 (s, 1H).

Synthesis of [Dy(L_{NN})(H₂O)₆]Cl₂·2H₂O (1). A solution of 0.5 mmol of the ligand HL_{NN} (0.113 g, 1 equivalent) and 0.5 mmol of triethylamine (0.13 mL, 1 equivalent) was left stirring for 5 min. The solution was then added dropwise for 10 min with stirring to a solution containing 0.5 mmol of DyCl₃·6H₂O (0.186 g, 1 equivalent) in 10 mL of methanol. The mixture was then left under stirring for 6h. After 4 days of slow evaporation of the solvent, crystals in the form of yellow needles were formed (yield 52%).

Synthesis of [Dy(L_{NN})₂(MeOH)₂(H₂O)₂]Cl (2). In a 25 mL flask containing 0.5 mmol of DyCl₃·6H₂O (0.186 g, 1 equivalent) and 1 mmol of HL_{NN} (0.226 g, 2 equivalents) in 15 mL of methanol, was added with magnetic stirring 1.5 mmol of triethylamine (0.26 mL, 3 equivalents). The mixture was then placed under reflux. After 3h, a light orange precipitate was formed. The latter was filtered and washed thoroughly with methanol and then solubilized in 10 mL of dichloromethane. After slow evaporation of the solvent, yellowish crystals were isolated (Yield 48%).

Synthesis of [Dy(L_{NN})₃(MeOH)₂] (3). To a suspension of 0.5 mmol of DyCl₃·6H₂O (0.186 g, 1 equivalent) and 1 mmol of HL_{NN} (0.226 g, 2 equivalents) in 5 mL of methanol was added 1.5 mmol of triethylamine (0.26 mL, 3 equivalents). As soon as the base was added, the resulting solution becomes clear yellow after 20 minutes of magnetic stirring. The solvent was then slowly evaporated. After 2 days, crystals in the form of thin needles were harvested (yield 71%).

Synthesis of {Dy(L_{NN})₃(MeOH)}_n (4). 8 mL of methanol, 0.5 mmol of DyCl₃·6H₂O (0.186 g, 1 equivalent), 1 mmol of HL_{NN} (0.226 g, 2 equivalents) and 1.5 mmol of triethylamine (0.26 mL, 3 equivalents) were introduced into a Teflon bomb. The support was then placed in a stainless steel autoclave. In an oven, the mixture was heated at 80°C for 12h. A crystalline powder was then recovered from the reaction medium by filtration. The solid was recrystallized from THF to give crystals in the form of thin yellowish needles (yield 56%).

Crystallography. Single-crystal X-ray studies of complexes **1-4** were carried out by using a Gemini diffractometer and the related analysis software, respectively.^[16] An absorption correction based on the crystal faces was applied to the data sets (analytical).^[17] The structures were solved by direct methods using the SIR97 program^[18] combined with Fourier difference syntheses and refined against F using reflections with $|\frac{I}{\sigma(I)}| > 3$ by using the CRYSTALS program.^[19] All atomic displacement parameters for non-hydrogen atoms were refined with anisotropic terms. The hydrogen atoms were theoretically located on the basis of the conformation of the supporting atom and refined by using the riding model. CCDC-1574559-1574562 contains the supplementary crystallographic data for this paper. These data can be obtained free of charge from The Cambridge Crystallographic Data Centre via www.ccdc.cam.ac.uk/data_request/cif. X-ray crystallographic data and refinement details for complexes **1-4** are summarized in

Supplementary Information Table SI.1. Important bond lengths, bond angles as well as intra- and inter-complexes distances are collated in Tables SI.2-SI.5.

Magnetic measurements.

Magnetic susceptibility data (2-300 K) were collected on powdered polycrystalline samples on a Quantum Design MPMS-XL SQUID magnetometer under an applied magnetic field of 1 kOe, using eicosane matrix to prevent sample reorientation during the measurement. Alternating current (ac) measurements were performed in the 2-12 K range of an ac driving field oscillating frequencies in 1-1300 Hz range. Magnetization isotherms were collected at 2 K. All data were corrected for the contribution of the sample holder and the diamagnetism of the samples estimated from Pascal's constants.

Ab initio calculations. Wavefunction-based calculations were carried out on complexes **1 - 4** by using the SA-CASSCF/RASSI-SO approach, as implemented in the MOLCAS quantum chemistry package (versions 8.0).^[20] The relativistic effects are treated in two steps on the basis of the Douglas-Kroll Hamiltonian. First, the scalar terms were included in the basis-set generation and were used to determine the spin-free wavefunctions and energies in the complete active space self-consistent field (CASSCF) method.^[21] Next, spin-orbit coupling was added within the restricted-active-space-state-interaction (RASSI-SO) method, which uses the spin-free wavefunctions as basis states.^[22] The resulting wavefunctions and energies are used to compute the magnetic properties and g-tensors of the lowest states from the energy spectrum by using the pseudo-spin $S = 1/2$ formalism in the SINGLE-ANISO routine.^[23] Cholesky decomposition of the bielectronic integrals was employed to save disk space and speed-up the calculations.^[24] The active space of the self-consistent field (CASSCF) method consisted of the nine 4f electrons of the Dy(III) ion spanning the seven 4f orbitals, i.e. CAS(9,7)SCF. State-averaged CASSCF calculations were performed for all of the sextets (21 roots), all of the quadruplets (224 roots), and 300 out of the 490 doublets of the Dy(III) ion. Twenty-one sextets, 128 quadruplets, and 107 doublets were mixed through spin-orbit coupling in RASSI-SO. All atoms were described by ANO-RCC basis sets. The following contractions were used: [8s7p4d3f2g1h] for Dy, [4s3p2d] for O, C and N atoms of the first coordination sphere, [3s2p] for the other N, C atoms, [5s4p2d1f] for Cl and [2s] for the H atoms. In the case of **4**, the chain structure was modeled using point charges computed on the molecular fragment within the LoProp approach,^[25] following a strategy successfully used previously.^[26] The atomic positions were extracted from the X-ray crystal structures. Only the positions of the H atoms were optimized on the Y analogues with the Gaussian 09 (revision D.01) package^[27] employing the PBE0 hybrid functional.⁸ The "Stuttgart/Dresden" basis sets and effective core potentials were used to describe the yttrium atom,^[28] whereas all other atoms were described with the SVP basis sets.^[29]

Acknowledgements

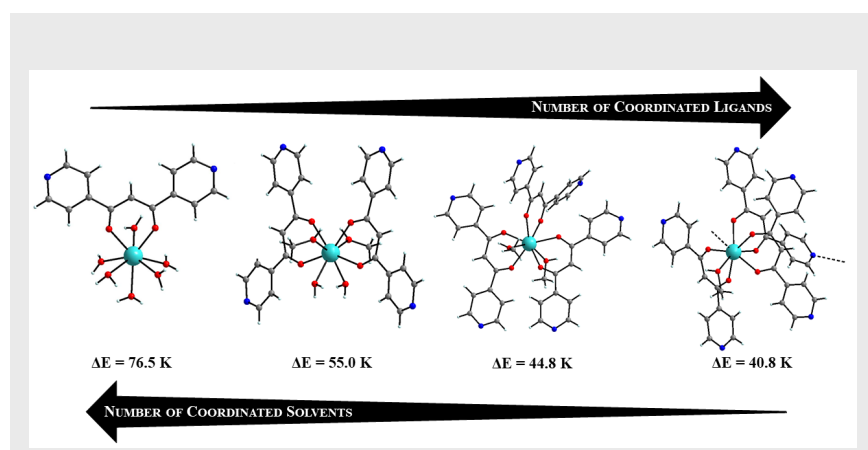
D. G. is grateful for the PhD fellowship from University Claude Bernard Lyon 1. Additional support was provided by the Région Rhône-Alpes (CMIRA2015). G. F. G. gratefully acknowledges the European Commission through the ERC-AdG 267746 MolNanoMas (project no. 267746) and the ANR (ANR-13-BS07-0022-01) for financial supports. B.L.G. thanks the French GENCI/IDRIS-CINES centre for high-performance computing resources.

Keywords: Dysprosium • SMM • Crystal structures • Magnetism • *ab initio* calculations

- [1] (a) A. Caneschi, D. Gatteschi, R. Sessoli, A.-L. Barra, L.C. Brunel, M. Guillot, *J. Am. Chem. Soc.* **1991**, *113*, 5873-5874; (b) R. Sessoli, D. Gatteschi, A. Caneschi, M. A. Novak, *Nature* **1993**, *365*, 141-143.
- [2] (a) F. Pointillart, O. Cador, B. Le Guennic, L. Ouahab *Coord. Chem. Rev.* **2017**, *346*, 150-175; (b) H. L. C. Feltham, S. Brooker, *Coord. Chem. Rev.* **2014**, *276*, 1-29; (c) P. Zhang, Y.-N. Guo, J. Tang, *Coord. Chem. Rev.* **2013**, *257*, 1728-1763; (d) F. Pointillart, B. Le Guennic, O. Cador, O. Maury, L. Ouahab, *Acc. Chem. Res.* **2015**, *48*, 2834-2842; (e) D. N. Woodruff, R. E. P. Winpenny, R. A. Layfield, *Chem. Rev.* **2013**, *113*, 5110-5148; (f) R. A. Layfield, *Organometallics*, **2014**, *33*, 1084-1099
- [3] (a) R. Sessoli, A. K. Powell, *Coord. Chem. Rev.* **2009**, *253*, 2328-2341; (b) L. Sorace, C. Benelli, D. Gatteschi, *Chem. Soc. Rev.* **2011**, *40*, 3092-3104.
- [4] (a) U. J. Williams, B. D. Mahoney, P. T. DeGregorio, P. J. Carroll, E. Nakamaru-Ogiso, J. M. Kikkawa, E. J. Schelter, *Chem. Comm.* **2012**, *48*, 5593-5595; (b) S. Cardona-Serra, J. M. Clemente-Juan, E. Coronado, A. Gaita-Ariño, A. Camón, M. Evangelisti, F. Luis, M. J. Martínez-Pérez, J. Sesé, *J. of the Am. Chem. Soc.* **2012**, *134*, 14982-14990; (c) Y. Bi, Y.-N. Guo, L. Zhao, Y. Guo, S.-Y. Lin, S.-D. Jiang, J. Tang, B.-W. Wang, S. Gao, *Chem. Eur. J.* **2011**, *17*, 12476-12481; (d) T. T. da Cunha, J. Jung, M.-E. Boulon, G. Campo, F. Pointillart, C. L. M. Pereira, B. Le Guennic, O. Cador, K. Bernot, F. Pineider, S. Golhen, L. Ouahab, *J. of the Am. Chem. Soc.* **2013**, *135*, 16332-16335.
- [5] (a) F. Habib, M. Murugesu, *Chem. Soc. Rev.* **2013**, *42*, 3278-3288; (b) G. Cucinotta, M. Perfetti, J. Luzon, M. Etienne, P.-E. Car, A. Caneschi, G. Calvez, K. Bernot, R. Sessoli, *Angew. Chem. Int. Ed.* **2012**, *51*, 1606-1610; (c) D. N. Woodruff, R. E. P. Winpenny, R. A. Layfield, *Chem. Rev.* **2013**, *113*, 5110-5148.
- [6] G.-J. Chen, Y.-N. Guo, J.-L. Tian, J. Tang, W. Gu, X. Liu, S.-P. Yan, P. Cheng, D.-Z. Liao, *Chem. Eur. J.* **2012**, *18*, 2484-2487.
- [7] D. Aravena, E. Ruiz, *Inorg. Chem.* **2013**, *52*, 13770-13778.
- [8] A. Beziau, S. A. Baudron, M. W. Hosseini, *Dalton Trans.* **2012**, *41*, 7227-7234.
- [9] M. Llunell, D. Casanova, J. Cirera, J. M. Bofill, P. Alemany, S. Alvarez, SHAPE, v. 2.1, Barcelona, Spain, **2013**
- [10] (a) A. K. Mondal, H. S. Jena, A. Malviya, S. Konar, *Inorg. Chem.* **2016**, *55*, 5237-5244; (b) M. L. Kahn, J.-P. Sutter, S. Golhen, P. Guionneau, L. Ouahab, O. Kahn, D. Chasseau, *J. of the Am. Chem. Soc.* **2000**, *122*, 3413-3421; (c) M. L. Kahn, R. Ballou, P. Porcher, O. Kahn, J.-P. Sutter, *Chem. Eur. J.* **2002**, *8*, 525-531.
- [11] O. Kahn, *Molecular Magnetism* **1993**
- [12] H. Lueken, *Course of lectures on magnetism of lanthanide ions under varying ligand and magnetic fields*
- [13] (a) K. S. Cole, *J. Chem. Phys.* **1941**, *9*, 341; (b) S. M. J. Aubin, Z. Sun, L. Pardi, J. Krzystek, K. Folting, L.-C. Brunel, A. L. Rheingold, G. Christou, D. N. Hendrickson, *Inorg. Chem.* **1999**, *38*, 5329-5340.
- [14] (a) J. Long, J. Rouquette, J.-M. Thibaud, R. A. S. Ferreira, L. D. Carlos, B. Donnadieu, V. Vieru, L. F. Chibotaru, L. Konczewicz, J. Haines, Y. Guari, J. Larionova, *Angew. Chem. Int. Ed.* **2015**, *127*, 2264-2270; (b) J.-B. Peng, Y.-P. Ren, X.-J. Kong, L.-S. Long, R.-B. Huang, L.-S. Zheng, *CrystEngComm* **2011**, *13*, 2084-2090.
- [15] (a) A. Lunghi, F. Totti, R. Sessoli, S. Sanvito, *Nature Commun.* **2017**, *8*, 14620; (b) C. A. P. Goodwin, F. Ortu, D. Reta, N. F. Chilton, D. P. Mills, *Nature*, **2017**, *548*, 439-442
- [16] CrysAlisPro, v. 1.171.33.46 (rel. 27-08-2009 CrysAlis171.NET), Oxford Diffraction Ltd., **2009**
- [17] (a) J. Demeulenaer, H. Tompa, *Acta Crystallographica* **1965**, *19*, 1014-1018; (b) R. H. Blessing, *Acta Crystallographica Section A* **1995**, *51*, 33-38.
- [18] A. Altomare, M. C. Burla, M. Camalli, G. L. Casciarano, C. Giacovazzo, A. Guagliardi, A. G. G. Moliterni, G. Polidori, R. Spagna, *Journal of Applied Crystallography* **1999**, *32*, 115-119.
- [19] D. J. Watkin, Prout, C. K., Carruthers, J. R., Betteridge, P. W. in CRISTAL Issue 11, Vol. CRISTAL Issue 11, Chemical Crystallography Laboratory, Oxford, UK, **1999**.
- [20] F. Aquilante, L. De Vico, N. Ferré, G. Ghigo, P.-A. Malmqvist, P. Neogady, T. B. Pedersen, M. Pitonak, M. Reiher, B. O. Roos, L. Serrano-Andrés, M. Urban, V. Veryazov, R. Lindh, *J. Comput. Chem.* **2010**, *31*, 224-247.
- [21] B. O. Roos, P. R. Taylor, P. E. M. Siegbahn, *Chem. Phys.* **1980**, *48*, 157.
- [22] (a) P.-A. Malmqvist, B. O. Roos, B. Schimmelpfennig, *Chem. Phys. Lett.* **2002**, *357*, 230-240. (b) P.-A. Malmqvist, B. O. Roos, *Chem. Phys. Lett.* **1989**, *155*, 189-194.
- [23] (a) L. F. Chibotaru, L. Ungur, *J. Chem. Phys.* **2012**, *137*, 064112; (b) L. F. Chibotaru, L. Ungur, A. Soncini, *Angew. Chem., Int. Ed.* **2008**, *47*, 4126-4129.
- [24] F. Aquilante, P.-A. Malmqvist, T. B. Pedersen, A. Ghosh, B. O. Roos, *J. Chem. Theory Comput.* **2008**, *4*, 694-702.
- [25] L. Gagliardi, R. Lindh and G. Karlstrom, *J. Chem. Phys.*, **2004**, *121*, 4494-4500.
- [26] J. Jung, F. Le Natur, O. Cador, F. Pointillart, G. Calvez, C. Daiguebonne, O. Guillou, T. Guizouarn, B. Le Guennic, K. Bernot, K. Kobayashi, J. Normand, K. Raghavachari, A. Rendell, J. C. Burant, S. S. Iyengar, J. Tomasi, M. Cossi, N. Rega, J. M. Millam, M. Klene, J. E. Knox, J. B. Cross, V. Bakken, C. Adamo, J. Jaramillo, R. Gomperts, R. E. Stratmann, O. Yazyev, A. J. Austin, R. Cammi, C. Pomelli, J. W. Ochterski, R. L. Martin, K. Morokuma, V. G. Zakrzewski, G. A. Voth, P. Salvador, J. J. Dannenberg, S. Dapprich, A. D. Daniels, O. Farkas, J. B. Foresman, J. V. Ortiz, J. Cioslowski, and D. J. Fox, Gaussian, Inc., Wallingford CT, **2013**
- [27] Gaussian 09, Revision D.01, M. J. Frisch, G. W. Trucks, H. B. Schlegel, G. E. Scuseria, M. A. Robb, J. R. Cheeseman, G. Scalmani, V. Barone, B. Mennucci, G. A. Petersson, H. Nakatsuji, M. Caricato, X. Li, H. P. Hratchian, A. F. Izmaylov, J. Bloino, G. Zheng, J. L. Sonnenberg, M. Hada, M. Ehara, K. Toyota, R. Fukuda, J. Hasegawa, M. Ishida, T. Nakajima, Y. Honda, O. Kitao, H. Nakai, T. Vreven, J. A. Montgomery, Jr., J. E. Peralta, F. Ogliaro, M. Bearpark, J. J. Heyd, E. Brothers, K. N. Kudin, V. N. Staroverov, T. Keith, R. Kobayashi, J. Normand, K. Raghavachari, A. Rendell, J. C. Burant, S. S. Iyengar, J. Tomasi, M. Cossi, N. Rega, J. M. Millam, M. Klene, J. E. Knox, J. B. Cross, V. Bakken, C. Adamo, J. Jaramillo, R. Gomperts, R. E. Stratmann, O. Yazyev, A. J. Austin, R. Cammi, C. Pomelli, J. W. Ochterski, R. L. Martin, K. Morokuma, V. G. Zakrzewski, G. A. Voth, P. Salvador, J. J. Dannenberg, S. Dapprich, A. D. Daniels, O. Farkas, J. B. Foresman, J. V. Ortiz, J. Cioslowski, and D. J. Fox, Gaussian, Inc., Wallingford CT, **2013**
- [28] M. Dolg, H. Stoll, H. Preuss, *Theor. Chim. Acta* **1993**, *85*, 441-450.
- [29] F. Weigend, R. Ahlrichs, *Phys. Chem. Chem. Phys.* **2005**, *7*, 3297-3305.

Entry for the Table of Contents

FULL PAPER

**Key Topic***

*D. Guettas, V. Montigaud, G. Fernandez Garcia, P. Larini, O. Cador, B. Le Guennic, G Pilet **

Page No. – Page No.

Fine control of metal environment within dysprosium-based mononuclear Single-Molecule Magnets